Thin Film Devices Materials

Proceedings of 6th Thin Film Materials & Devices Meeting
November 2-3, 2009, Kyoto, Japan
http://www.tfmd.jp/

Analysis of Impurity doping Using Free Carrier Absorption

T. Sameshima[(1)], K. Ukawa[(1)], N. Sano[(2)], M.Naito[(3)] and N. Hamamoto[(3)]
[(1)]Tokyo University of Agriculture and Technology, 2-24-16, Naka-cho, Koganei, Tokyo, 184-8588
[(2)]Hightec Systems Corporation, 3-9-15, Shin Yokohama, Kohoku-ku, Yokohama, Kanagawa, 222-0033
[(3)] Nissin Ion Equipment Co., Ltd. Koka, Shiga 528-0068, Japan
E-mail :tsamesim@cc.tuat.ac.jp

Keywords: free carrier absorption, carrier density, activation, laser annealing, optical interference, FTIR, ion implantation

Abstract.
We report analysis of activation of phosphorus atoms implanted into silicon. Phosphorus ions with 1×10^{15} cm^{-2} were implanted at 100 and 500 keV into p-type silicon samples. The samples were annealed by 976 nm semiconductor laser irradiation at 500 kW/cm^2 for 19~42 µs. These processes resulted in buried layers with a high density of electron free carriers. Measurements of infrared transmissivity showed oscillation spectra between 1000 and 7000 cm^{-1} because of optical interference effect due to change in refractive indexes induced by electron free carriers in the buried layers. Analysis of transmissivity spectra was conducted using a numerical program constructed with Fresnel coefficient and free carrier photo absorption theories. Activation initiated at deep region and proceeded to the surface as the laser dwell time increased in the case of implantation at 100 keV. On the other hand, activation occurred uniformly in depth direction for the every laser dwell time in the case of implantation at 500 keV.

Introduction

Free carrier photo absorption is useful for nondestructive investigation of electrical properties of semiconductor materials [1]. Free carriers change the effective dielectric constant as,

$$\varepsilon = \varepsilon_s \left(1 - \frac{\omega_p^2}{\omega^2}\frac{\omega^2\tau^2 + i\omega\tau}{\omega^2\tau^2 + 1}\right) \quad (1),$$

where ε_s is the intrinsic dielectric constant of materials, ω is the angular frequency of incident electromagnetic wave, τ is the lifetime of free carrier motion, and ω_p is the plasma frequency given as,

$$\omega_p = \sqrt{\frac{e^2 N}{m^* \varepsilon_s}} \quad (2),$$

Where, e is the elemental charge, N is the free carrier volume density, m^* is the effective mass of free carriers. When the effective dielectric constant is complexly expressed by $\varepsilon = \varepsilon_r - i\varepsilon_i$, the refractive index and extinction coefficient are respectively given as,

$$n = \sqrt{\frac{\varepsilon_r + \sqrt{\varepsilon_r^2 + \varepsilon_i^2}}{2\varepsilon_0}} \quad (3),$$

$$k = \frac{\varepsilon_i}{\sqrt{2\varepsilon_0}\sqrt{\varepsilon_r + \sqrt{\varepsilon_r^2 + \varepsilon_i^2}}} \quad (4),$$

where ε_0 is the dielectric constant in vacuum. Eqs.(3) and (4) mean that the refractive index and extinction coefficient depend on real and imaginary parts of the effective dielectric constant. They can be changed by exist of free carriers. Changes in n and k cause change in optical reflectivity and transmissivity of materials.

This paper reports analysis of activation of impurities formed by ion implantation followed by laser annealing using the free carrier absorption effect [2, 3]. When impurities implanted in deep regions are activated, buried layers with free carriers are formed in the deep regions. Free carriers cause change in the refractive index and extinction coefficient in the buried layers. On the other hand, the surface region keeps initial refractive index and extinction coefficient because of low impurity concentration. A layered structure with different refractive indexes and extinction coefficients is therefore formed by impurity ion implantation and its activation. Optical interference effect is caused by the layered structure of refractive index and extinction coefficient. We discuss analysis of the optical interference effect in the infrared range for samples with phosphorus atoms implanted at 100 and 500 keV and annealed by infrared semiconductor laser with different conditions.

Analysis

Free carrier optical absorption effect was calculated in the case of electron free carriers which distributed like Gaussian shape in depth with different peaks and widths in crystalline silicon. The carrier mobility μ was given according to the carrier density [4]. The carrier lifetime τ was defined as $\tau = m^*\mu/e$. We constructed a numerical analysis program combining finite element Fresnel coefficient method with free carrier effect shown in Eqs. (1)~(4) in order to calculate transmittance spectra in the infrared range [5]. Figure 1 shows transmissivity spectra calculated with a total electron carrier density of 1×10^{15} cm^{-2}, a peak width of 50 nm, and different depths of carrier density peak ranging from 50 to 600 nm (a), and difference in transmissivity spectra obtained by subtracting spectrum of undoped silicon from the spectra shown in Fig. 2(a), (b). Every spectrum in Fig. 1(a) showed marked decrease in transmissivity in wavelength lower than 1000 cm^{-1} because of substantial free carrier optical absorption. Oscillating line shapes owing to optical interference effect were observed in wavelength between 1000 and 7000 cm^{-1}, as shown in Fig. 1(b). When free carriers located in shallow

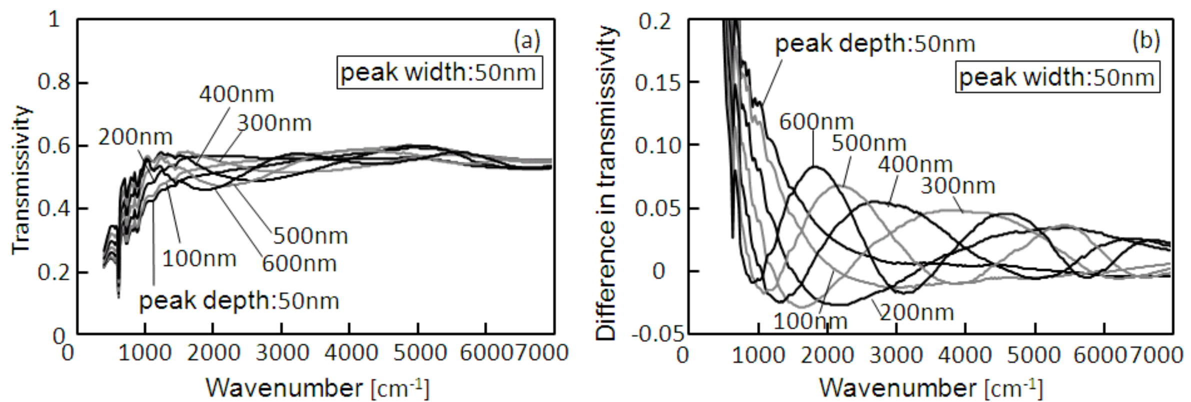

Fig. 1 Transmissivity spectra calculated with a total electron carrier density of 1×10^{15} cm^{-2}, a peak width of 50 nm, and different depths of carrier density peak ranging from 50 to 600 nm (a), and difference in transmissivity spectra obtained by subtracting spectrum of undoped silicon from spectra (b).

regions, valleys and peaks appeared only in high wavenumbers because the thin region at the surface with intrinsic refractive index allowed the optical resonance condition only for light with high wavenumbers and low wavelengths. On the other hand, when free carriers located in deep regions, many valleys and peaks appeared because the thick surface region with intrinsic refractive index allowed the optical resonance condition even for infrared light with low wavenumbers. Figure 2 shows calculated difference in transmissivity spectra obtained by subtracting spectrum of undoped silicon from spectra calculated with a total electron carrier density of $1x10^{15}$ cm^{-2}, a peak depth of 600 nm, and different widths ranging from 50 to 500 nm. Three valleys and peaks appeared in spectra between 1000 and 7000 cm^{-1} for every condition. Height of valleys and peaks in high wavenumber regions markedly decreased as the peak width increased. Moreover, the wavenumber of valleys and peaks in low wavenumber regions slightly decreased as the peak width increased. Those calculations indicate that transmissivity spectra sensitively change with distribution of free carriers in buried regions.

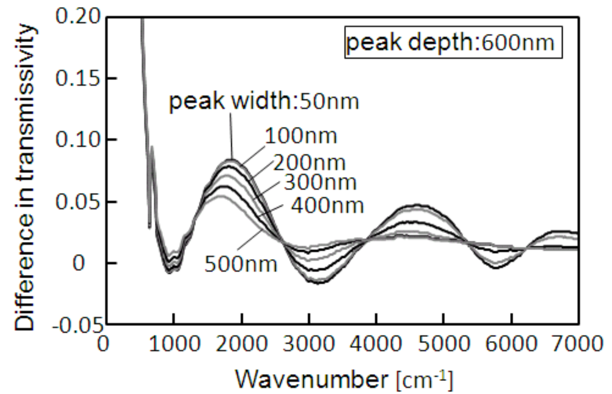

Fig. 2 calculated difference in transmissivity spectra obtained by subtracting spectrum of undoped silicon from spectra calculated with a of $1x10^{15}$ cm^{-2} carrier density, a peak depth of 600 nm, and different widths.

Experimental

Phosphorus atoms with a concentration of $1x10^{15}$ cm^{-2} were implanted at 100 and 500 keV to 20 Ωcm P-type silicon substrates. Measurements of optical reflectivity spectra in ultra violet and visible ranges revealed that the top 140 nm surface region was amorphized in the case of implantation at 100 keV, and that there was no substantial amorphous region in the case of implantation at 500 keV [6]. 200 nm thick carbon photo absorption layers were formed on the silicon surface by sputtering method. Continuous wave 976 nm semiconductor laser were irradiated to the carbon surface at 500 kW/cm^2 for 19~42 μs [7]. Figure 3 shows phosphorus in-depth profiles measured by secondary ion mass spectroscopy (SIMS) for samples implanted at 100 and 500 keV and samples laser annealed for 42 μs. SIMS showed almost the same in-depth profiles between samples as-implanted at 100 and 500 keV and samples laser annealed, respectively. There was no substantial diffusion of phosphorus atoms induced by laser annealing. The phosphorus concentration had a peak of 125 nm and a width of 135 nm in the case of implantation at 100 keV. It had a peak of 600 nm and a width of 360 nm in the case of implantation at 500 keV. Carbon layers were removed by oxygen plasma treatment after laser annealing. The rear surface was

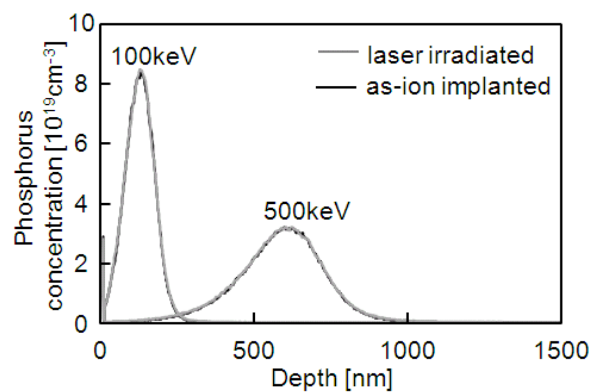

Fig. 3 phosphorus in-depth profiles for samples implanted at 100 and 500 keV and samples laser annealed for 42 μs.

polished to a mirror surface for optical transmissivity measurement using Fourier transfer infrared spectroscopy.

Results and discussion

Figure 4 shows transmissivity spectra for samples implanted at 100 keV (a) and 500 keV (b), which were heated by laser irradiation for 25~42 μs. Sheet resistivity was also presented in the figures. The transmissivity lower than 2500 cm^{-1} decreased as laser dwell time increased for samples implanted at 100 and 500 keV. In addition, decrease in transmissiviy around 2000 cm^{-1} was observed for samples implanted at 500 keV. The sheet resistivity decreased as the laser dwell time increased for the both implantation conditions. Figure 5 shows difference in transmissivity spectra obtained by subtracting spectrum of undoped silicon from spectra shown in Fig. 4. In the case of implantation at 100 keV, difference in transmissivity below 2500 cm^{-1} was low and a valley and peak appeared at 2700 and 5500 cm^{-1} for laser annealing for 25 μs. Difference in transmissivity below 2500 cm^{-1} increased as the laser dwell time increased because of substantial free carrier absorption. The valley and peak shifted to higher wavenumber as the laser dwell time increased. Those shifts mean that the free carrier region moved near the surface as the laser dwell time increased. On the other hand, in the case of implantation at 500 keV, large transmissivity difference was observed for every laser dwell time. Moreover, samples annealed with different laser dwell times showed similar spectral line shape. There were valleys at 1000, 3000 and 5600 cm^{-1}, and peaks at 1800 and 4300 cm^{-1}. The peak height at 1800 cm^{-1} increased. It means that the carrier density increased as the laser dwell time increased.

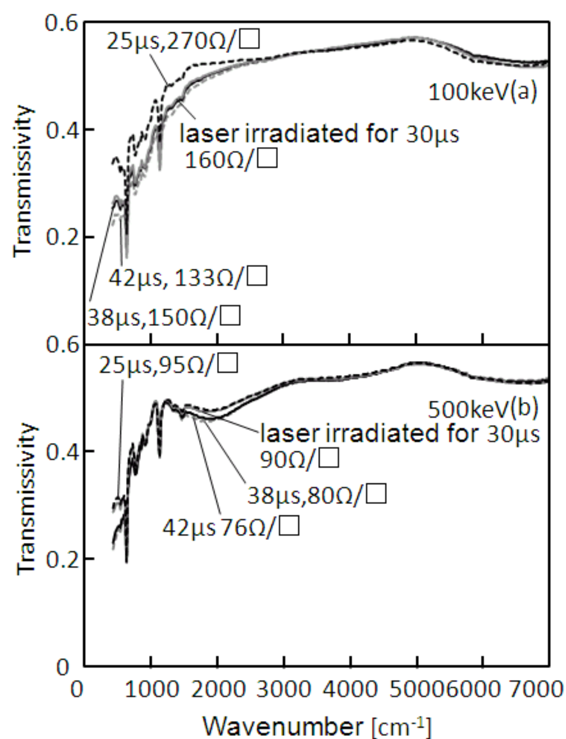

Fig. 4 Transmissivity spectra for samples implanted at 100 keV (a) and 500 keV (b), which were heated by laser irradiation for 25~42 μs.

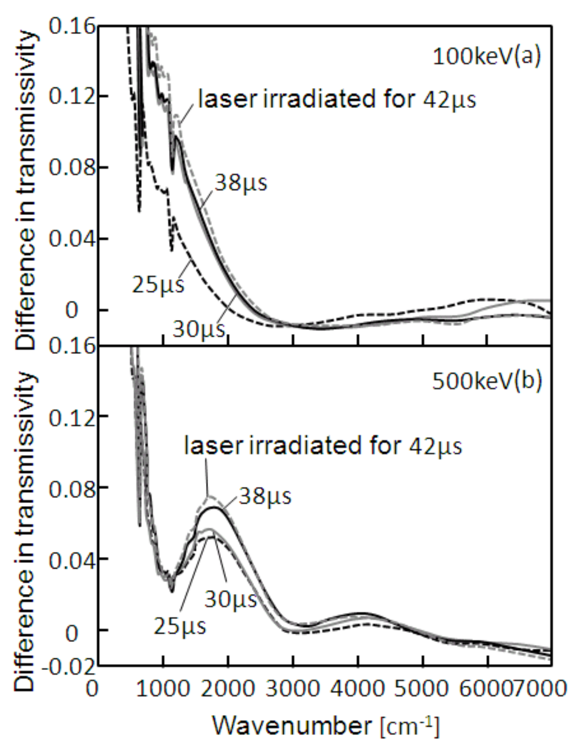

Fig. 5 Differences in transmissivity spectra obtained by subtracting spectrum of undoped silicon from spectra shown in Fig. 4 for samples implanted at 100 keV (a) and 500 keV (b).

We analyzed experimental spectra shown in Fig. 5 with our numerical calculation program. Figure 6 shows carrier in-depth profiles prepared for fitting experimental spectra for implanted 100 keV (a) and 500 keV (b). And figure 7 shows deference in tansmissivity spectra calculated using carrier in-depth profiles shown in Fig. 6. Shallow carrier localization shown in Fig. 6(a) resulted in broad spectra as shown in Fig. 7(a). Laser dwell time for 25 μs resulted in carrier location around 180 nm in deep, which gave a valley at low wavenumber in difference in transimissivity spectra as shown in Fig. 7(a). Laser dwell time for 42 μs resulted in carrier distribution from surface to 200 nm, which gave a valley at high wavenumber in difference in transimissivity spectra as shown in Fig. 7(a). This means that impurity activation initiated from deep regions, and that it proceeded to the surface as the laser dwell time increased. The surface 140 nm region was amorphized by implantation at 100 keV. Recrystallization was necessary to generate high density free carrier. The results of Figs. 6 and 7 indicate that recrystallization proceeded from the deep region to the surface region with increasing the laser dwell time. On the other hand, similar carrier in-depth profiles were used for fitting experimental spectra for every laser dwell time in the case of implantation at 500 keV, as shown in Fig. 6(b). This indicates that uniform activation in-depth direction occurred for every laser dwell time. Crystalline state was kept after phosphorus ion implantation at 500 keV. Uniform activation would be possible because silicon substrate is heated to high temperature in 30 μm deep regions at least during laser irradiation longer than 20 μs. Thermal energy for moving phosphorus atoms into silicon lattice sites was only necessary for activation. Long laser dwell time gave high enough energy to activate phosphorus atoms uniformly. Similar and deep carrier density profiles gave similar difference spectra in transmissivity with oscillation line shapes as shown in Fig. 7(b), which well explained the experimental spectra shown in Fig.

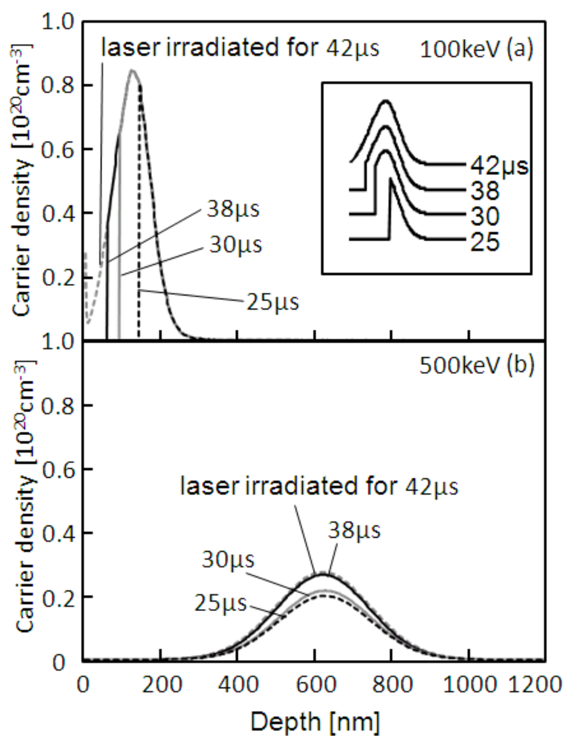

Fig. 6 Carrier density in-depth profiles used for fitting experimental spectra in the cases of 100 keV (a) and 500 keV (b) with different laser dwell times. Inset in (a) presents image of carrier in-depth profiles.

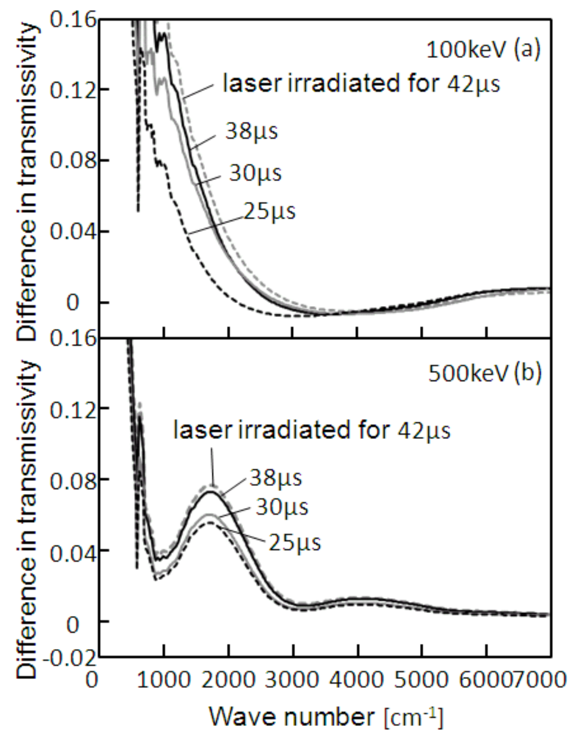

Fig. 7 Difference in transmissivity spectra obtained by subtracting spectrum of undoped silicon calculated using carrier density in-depth profile shown in Fig. 6.

5(b).

Figure 8 shows the total carrier density as a function of laser dwell time. In the case of implantation at 100 keV, the carrier density was very low of 1.4×10^{14} cm^{-2} for a laser dwell time of 19 μs. It increased to 1×10^{15} cm^{-2}, which was the same value of doping concentration. On the other hand, a carrier density of 4×10^{14} cm^{-2} was already observed for a laser dwell time of 19 μs in the case of implantation at 500 keV. It increased to 8×10^{14} cm^{-2}, which was lower than the implantation concentration, as the laser dwell time increased 42 μs

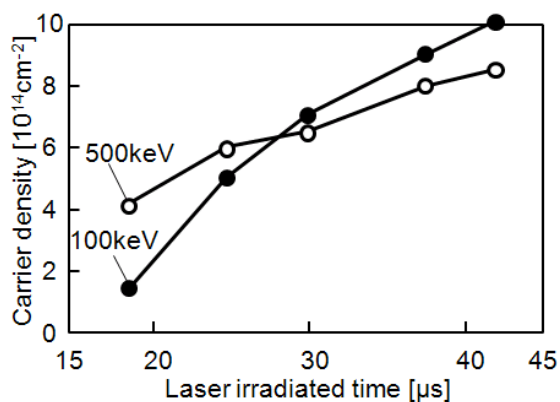

Fig. 8 carrier density as a function of laser dwell time for samples implanted at 300 and 500 keV.

Summary

We investigated activation behavior of phosphorus atoms implanted into silicon using numerical calculation program of transmissivity with finite element free carrier optical absorption and Fresnel coefficient interference models. Free carriers change refractive index and extinction coefficient. When they locate in deep regions, optical interference effect occurs among layers with different refractive indexes and extinction coefficients. Phosphorus ions with 1×10^{15} cm^{-2} were implanted at 100 and 500 keV into 20 Ωcm p-type silicon samples. 200 nm thick carbon optical absorption layers were then formed on the surface by sputtering. Samples were annealed by 976 nm semiconductor laser irradiation at 500 kW/cm^2 for 19~42 μs. Infrared transmissivity spectra of samples showed oscillation spectra between 1000 and 7000 cm^{-1} because of optical interference effect due to change in refractive indexes induced by electron free carriers. In the case of implantation at 100 keV, a valley and peak appeared at 2700 and 5500 cm^{-1} for laser annealing for 25 μs. The valley and peak shifted to higher wavenumber as the laser dwell time increased. Those shifts mean that the free carrier region moved near the surface as the laser dwell time increased. This revealed that activation proceeded from the deep region to the surface according to recrystallization. On the other hand, in the case of implantation at 500 keV, there were valleys at 1000, 3000 and 5600 cm^{-1}, and peaks at 1800 and 4300 cm^{-1} for every dwell time condition. This means that activation occurred uniformly in depth direction for the every laser dwell time in the case of implantation at 500 keV.

Acknowledgments

This work was partially supported by NEDO foundation P07026.

REFERENCES

[1] T. Sameshima, tutorial text in 6th Thin Film Materials & Devices Meeting (Kyoto, 2009).
[2] H. Engstrom: J. Appl. Phys. **51** (1980) 5245.
[3] T. Sameshima, K. Saitoh, N. Aoyama, S. Higashi, M. Kondo, and A. Matsuda: Jpn. J. Appl. Phys. **38**(1999)1892.
[3] M. J. Kerr and A. Cuevas: Semicond. Sci. Technol. **17**, (2002) 166.
[4] J. C. Irvin: Bell Syst. Tech. J. 41 (1962) 387.
[5] T. Sameshima, H. Hayasaka, and T. Haba, Jpn. J.Appl. Phys. 48 (2009) 021204-1-6.
[6] T. Sameshima, Y. Matsuda, Y.Andoh, and N. Sano, Jpn. J.Appl. Phys. 47 (2008) 1871.
[7] N. Sano, M. Maki, N. Andoh and T. Sameshima, Jpn. J. Appl. Phys. 46 (2007) 1254.